SIAM J. NUMER. ANAL.
Vol. 58, No. 6, pp. 3332–3354

NUMERICAL SIMULATION OF INEXTENSIBLE ELASTIC RIBBONS*

SÖREN BARTELS†

Abstract. Using dimensionally reduced models for the numerical simulation of thin objects is highly attractive as this reduces the computational work substantially. The case of narrow thin elastic bands is considered, and a convergent finite element discretization for the one-dimensional energy functional and a fully practical, energy-monotone iterative method for computing stationary configurations are devised. Numerical experiments confirm the theoretical findings and illustrate the qualitative behavior of elastic narrow bands.

Key words. elastic ribbons, finite element method, iterative solution, convergence

AMS subject classifications. 65N12, 65N30, 74B20, 74K20

DOI. 10.1137/20M1357494

1. Introduction.

Thin elastic objects provide a fascinating range of applications, particularly in nanotechnology, where small lightweight constructions can undergo large deformations that are controlled by external stimuli; cf., e.g., [15]. An important class of these objects is elastic ribbons, which are thin elastic bands of small width. A characteristic feature is that these bands are unshearable, and hence curvature can only occur orthogonally to the strip's inplane direction. A particular configuration that has been addressed in the literature is Möbius strips of small width; cf. [16, 14, 4].

To effectively simulate the highly nonlinear behavior of thin elastic objects, dimensionally reduced mathematical descriptions are necessary. In the case of ribbons a one-dimensional model has been proposed by Sadowsky in [12, 13] which was obtained via formal arguments; further justifications have been given in [16, 10]. A complete, mathematically rigorous derivation from three-dimensional hyperelasticity has been carried out in [6], which shows that a correction of Sadowsky's functional is necessary. The correction concerns the important case of vanishing curvature and thereby provides a more general description. Additionally, this eliminates a singularity in Sadowsky's functional which is particularly important for the stable discretization and iterative solution. The nonsmooth character of the corrected functional underlines the expected feature that the behavior of ribbons is substantially more complicated than that of elastic rods; cf. [11] for a corresponding rigorously derived mathematical model. Our numerical experiments confirm that the correction in the one-dimensional functional is relevant. A comparison of certain instabilities of twisted rods and ribbons is provided in [1]. The presence of such effects supports the importance of developing stable numerical approximation schemes.

The model identified in [6] describes the deformation of an elastic ribbon of length

*Received by the editors August 3, 2020; accepted for publication (in revised form) September 3, 2020; published electronically November 17, 2020.
https://doi.org/10.1137/20M1357494
Funding: The work of the author was supported by the Isaac Newton Institute for Mathematical Sciences program "Geometry, compatibility and structure preservation in computational differential equations," the EPSRC grant EP/R014604/1, and the German Research Foundation (DFG) via the research unit FOR 3013 "Vector- and tensor-valued surface PDEs."
†Abteilung für Angewandte Mathematik, Albert-Ludwigs-Universität Freiburg, Hermann-Herder-Str. 10, 79104 Freiburg i. Br., Germany (bartels@mathematik.uni-freiburg.de).

$L > 0$ via a frame (y, b, d) consisting of functions

$$y, b, d : (0, L) \to \mathbb{R}^3,$$

defined on the centerline $(0, L)$ of the undeformed ribbons. The frame condition requires the functions to satisfy

$$[y', b, d] \in SO(3)$$

pointwise in $(0, L)$ with the set of proper orthogonal matrices $SO(3)$. In particular, y provides an arclength parametrization of the deformed centerline. The arclength property $|y'|^2 = 1$ models the physical feature that thin elastic objects are inextensible in the bending regime. The directors b and d define the deformation of the band orthogonal to the centerline. Since the band cannot be sheared, the inplane curvature vanishes; i.e., the additional condition

$$y'' \cdot b = 0$$

occurs, which in view of the relation $y' \cdot b = 0$ is equivalent to the condition $y' \cdot b' = 0$. A frame (y, b, d) describing the deformation of an elastic band for given boundary conditions minimizes the dimensionally reduced elastic energy

$$E[y, b, d] = \int_0^L \overline{Q}(y'' \cdot d, b' \cdot d)\, \mathrm{d}x,$$

where

$$\overline{Q}(\alpha, \beta) = \begin{cases} (\alpha^2 + \beta^2)^2/\alpha^2 & \text{if } |\alpha| \geq |\beta|, \\ 4\beta^2 & \text{if } |\alpha| \leq |\beta|. \end{cases}$$

Appropriately scaled body forces can be included in the minimization problem. Because of the frame condition and the constraint $y'' \cdot b = 0$, the functional can be expressed in terms of the curvature κ and torsion τ of the curve parametrized by y and described by the frame (y, b, d). These quantities are given by

$$\kappa^2 = (y'' \cdot d)^2 = |y''|^2, \quad \tau^2 = (b' \cdot d)^2 = |b'|^2,$$

and we may consider the equivalent functional

$$E[y, b] = \int_0^L \overline{Q}(|y''|, |b'|)\, \mathrm{d}x.$$

The omitted director d can be reconstructed via $d = y' \times b$.

Various aspects of the outlined variational problem make the numerical approximation of minimizers difficult. First, the function $\overline{Q}$ is convex and continuously differentiable but not twice continuously differentiable. Hence, to apply iterative solution techniques, regularizations are required. Second, the nonlinear pointwise constraints have to be discretized appropriately and incorporated into the solution strategy. Third, the nonlinear dependence of the integrand on highest derivatives complicates the analysis of quadrature effects. Fourth, the iterative minimization has to be carefully done to reliably decrease the energy and avoid the occurrence of irregular stationary configurations.

We devise a discretization of E that uses piecewise cubic, C^1 conforming finite elements for the approximation of y, and piecewise linear, C^0 conforming finite elements

for b. The variable d is eliminated via the relation $d = y' \times b$. A twice continuously differentiable regularization $\overline{Q}_\delta$ of $\overline{Q}$ is used, and the orthogonality relations $y' \cdot b = 0$ and $y' \cdot b' = 0$ are incorporated using penalization; i.e., we consider

$$E_{\delta,\varepsilon,h}[y_h, b_h] = \int_0^L \overline{Q}_\delta(|y_h''|, |b_h'|)\,\mathrm{d}x + \frac{1}{2\varepsilon_1}\int_0^L (y_h' \cdot b_h)^2\,\mathrm{d}x + \frac{1}{2\varepsilon_2}\int_0^L (y_h' \cdot b_h')^2\,\mathrm{d}x.$$

The unit length conditions $|y'|^2 = 1$ and $|b|^2 = 1$ are imposed at the nodes of the partitioning defining the finite element spaces; i.e.,

$$\mathcal{I}_h^{1,0}|y_h'|^2 = \mathcal{I}_h^{1,0}|b_h|^2 = 1$$

with the nodal interpolation operator $\mathcal{I}_h^{1,0}$ related to piecewise linear, continuous finite element functions. We derive three convergence results for the discretized functional and its minimizers. By employing a recent structure-preserving density result from [9] for framed curves, we rigorously establish that the functionals $E_{\delta,\varepsilon,h}$ are Γ-convergent to the corrected Sadowsky functional as $(\delta, \varepsilon, h) \to 0$ under appropriate scaling relations. A generalization of the results based on Jensen's inequality includes the use of quadrature in nonquadratic terms, which makes the devised method fully practical even in the case of minimal regularity properties. A justification of clamped boundary conditions in the dimensionally reduced model is currently under investigation [7].

The discretized elastic energies $E_{\delta,\varepsilon,h}$ are particularly suitable for the minimization using gradient flows, i.e., a discrete version of the formal evolution equations

$$\partial_t y = -\nabla_y E[y, b] + (\lambda y')', \quad \partial_t b = -\nabla_b E[y, b] - \mu b,$$

for given initial and boundary data and suitable definitions of the gradients with respect to the variables y and b. The Lagrange multipliers λ and μ correspond to the pointwise unit length constraints. To define a discrete variant we use a splitting of the (regularized) energy density $\overline{Q}_\delta$ into quadratic and nonlinear parts; i.e., we have

$$\overline{Q}_\delta(\alpha, \beta) = \frac{1}{2}\alpha^2 + \frac{5}{2}\beta^2 + \psi_\delta(\alpha^2, \beta^2).$$

With backward difference quotient operator d_t to approximate the time derivatives and suitable implicit and explicit treatments of variations of the discrete energy $E_{\delta,\varepsilon,h}$, the time stepping scheme reads

$$\begin{aligned}(d_t y_k, w)_\star + (y_k'', w'') + \varepsilon_1^{-1}(y_k' \cdot b_{k-1}, w' \cdot b_{k-1}) + \varepsilon_2^{-1}(y_k' \cdot b_{k-1}', w' \cdot b_{k-1}') \\ = -(\psi_{\delta,1}'(|y_{k-1}''|^2, |b_{k-1}'|^2) y_{k-1}'', w''), \\ (d_t b_k, r)_\dagger + 5(b_k', r') + \varepsilon_1^{-1}(y_k' \cdot b_k, y_k' \cdot r) + \varepsilon_2^{-1}(y_k' \cdot b_k', y_k' \cdot r') \\ = -(\psi_{\delta,2}'(|y_{k-1}''|^2, |b_{k-1}'|^2) b_{k-1}', r'),\end{aligned}$$

subject to linearized pointwise constraints

$$d_t y_k' \cdot y_{k-1}' = 0, \quad d_t b_k \cdot b_{k-1} = 0.$$

The equations are linear and decoupled in the variables y_k and b_k. The inner products $(\cdot,\cdot)_\star$ and $(\cdot,\cdot)_\dagger$ have to be sufficiently strong in order to control certain discretization

errors avoiding restrictive step size restrictions. For this decoupling the penalized approximation of the orthogonality relations using separately convex functionals is essential. We show that the resulting discrete time stepping scheme is energy decreasing and that the violation of the constraints is controlled uniformly. For related results for bending-torsion models for elastic rods we refer the reader to [5].

An alternative approach to the numerical simulation of elastic ribbons is obtained by discretizing the two-dimensional nonlinear plate bending model from [8] and the finite element method devised in [2, 3]. This has the disadvantage of discretizing a two-dimensional domain but the advantages that the model leads to the constrained minimization of a quadratic functional and incorporates the width parameter, which may be relevant in certain applications. However, the explicit occurrence of the width requires the use of very fine discretizations.

The outline of this article is as follows. We specify employed notation and elementary facts about finite element methods in section 2. The continuous variational problem and its regularized approximation are addressed in section 3. In section 4 we define a discrete approximation of the regularized variational problem and investigate its convergence to the continuous one. A discrete gradient flow is devised and analyzed in section 5. Numerical experiments are reported in section 6.

2. Preliminaries.

2.1. Lebesgue and Sobolev spaces. Throughout this article we use standard notation for Sobolev and Lebesgue spaces. We abbreviate the L^2 norm via

$$\|\cdot\| = \|\cdot\|_{L^2(0,L)}.$$

Throughout we use standard embedding results, e.g., that $H^1(0,L)$ is compactly embedded in $C^0(0,L)$.

2.2. Finite element spaces. We always let $\mathcal{T}_h$ denote a partitioning $x_0 < x_1 < \cdots < x_N$ of the interval $(0,L)$ into elements $T_j = [x_{j-1}, x_j]$, $j = 1, 2, \ldots, N$, with maximal mesh-size $h = \max_{j=1,\ldots,N} h_{T_j}$ with $h_{T_j} = |x_j - x_{j-1}|$. Sets of piecewise polynomial functions of degree at most p and which are k times continuously differentiable are denoted by the sets

$$\mathcal{S}^{p,k}(\mathcal{T}_h) = \big\{v_h \in C^k(0,L) : v_h|_T \in P_p(T) \text{ for all } T \in \mathcal{T}_h\big\}.$$

Associated with these spaces is a nodal interpolation operator

$$\mathcal{I}_h^{p,k} : C^k(0,L) \to \mathcal{S}^{p,k}(\mathcal{T}_h).$$

We work with the spaces $\mathcal{S}^{1,0}(\mathcal{T}_h)$ of piecewise linear, globally continuous functions and $\mathcal{S}^{3,1}(\mathcal{T}_h)$ of piecewise cubic, globally continuously differentiable functions for which the interpolation operators are entirely determined by the conditions

$$\mathcal{I}_h^{1,0} v(x_j) = v(x_j)$$

and

$$\mathcal{I}_h^{3,1} w(x_j) = w(x_j), \quad \big(\mathcal{I}_h^{3,1} w\big)'(x_j) = w'(x_j)$$

for $v \in C^0([0,L])$ and $w \in C^1([0,L])$ and $j = 0, 1, \ldots, N$, respectively. The operators satisfy the estimates

$$\|v - \mathcal{I}_h^{1,0} v\|_{H^r(0,L)} \le c_{1,0} h^{2-r} \|v''\|$$

for $r = 0, 1$, and

$$\|w - \mathcal{I}_h^{3,1} w\|_{H^r(0,L)} \le c_{3,1} h^{3-r} \|w^{(3)}\|$$

for $r = 1, 2$, respectively. Moreover, $\|(\mathcal{I}_h^{3,1} w)'''\|_{L^2(T)} \le c'_{3,1} \|w^{(3)}\|_{L^2(T)}$ for all $T \in \mathcal{T}_h$ and $w \in H^3(T)$. We also note the inverse estimate

$$\|v_h\|_{L^\infty(T)} \le c_{\mathrm{inv}} h_T^{-1/2} \|v_h\|_{L^2(T)} \tag{1}$$

for all $T \in \mathcal{T}_h$ and $v_h \in P_p(T)$ with a constant c_{inv} depending on the polynomial degree p. We will always assume that the partitioning $\mathcal{T}_h$ is quasiuniform so that the minimal mesh-size is comparable to the maximal mesh-size, i.e., $\min_{T \in \mathcal{T}_h} h_T \ge ch$.

2.3. Difference quotients. Given a step size $\tau > 0$ and an arbitrary sequence $(a^k)_{k=0,\dots,K}$, the backward difference quotient $d_t a^k$ is for $k = 1, 2, \dots, K$ defined via

$$d_t a^k = \tau^{-1}\big(a^k - a^{k-1}\big).$$

A binomial formula implies the identity

$$d_t a^k \cdot a^k = \frac{1}{2} d_t |a^k|^2 + \frac{\tau}{2} |d_t a^k|^2. \tag{2}$$

2.4. Γ convergence. We use the concept of Γ convergence to justify discretizations $(E_h)_{h>0}$ of the functional E as $h \to 0$. The discrete and continuous functionals are defined on $V = H^2(0, L; \mathbb{R}^3) \times H^1(0, L; \mathbb{R}^3)$; infinite values are used to incorporate constraints and to formally extend the discrete functionals to the common domain V. The functionals E_h are Γ-convergent to E with respect to weak convergence in V if (i) for every $(y, b) \in V$ there exists a sequence $(y_h, b_h)_{h>0} \in V$ such that $(y_h, b_h) \rightharpoonup (y, b)$ in V and $\lim_{h\to 0} E_h[y_h, b_h] = E[y, b]$ as $h \to 0$, and (ii) for every bounded sequence $(y_h, b_h)_{h>0}$ in V with weak limit $(y, b) \in V$ we have $\liminf_{h\to 0} E_h[y_h, b_h] \ge E[y, b]$. If the functionals E_h also satisfy an equicoercivity property which implies the uniform boundedness of sequences of minimizers, then these conditions imply that minimizers or, more generally, almost-minimizers (y_h, b_h) for E_h weakly accumulate at minimizers for E.

3. Reduced model and regularized approximation.

3.1. Elastic ribbons. We consider a dimensionally reduced model for narrow ribbons rigorously derived in [6]. The one-dimensional variational problem is defined via the elastic energy

$$E[y, b] = \int_0^L \overline{Q}(|y''|, |b'|)\, \mathrm{d}x.$$

The vectors y', b, and $d = y' \times b$ are required to constitute an orthonormal frame, i.e.,

$$[y', b, d] \in SO(3),$$

almost everywhere in $(0, L)$. This implies that y and b satisfy the constraints

$$|y'|^2 = 1, \quad |b|^2 = 1, \quad y' \cdot b = 0.$$

Moreover, the derivation of the model leads to the constraint that the inplane curvature component vanishes; i.e.,

$$y'' \cdot b = 0,$$

which in view of $y' \cdot b = 0$ is equivalent to $y' \cdot b' = 0$. The function $\overline{Q}$ is given by

$$\overline{Q}(\alpha,\beta) = \begin{cases} (\alpha^2+\beta^2)^2/\alpha^2 & \text{if } |\alpha| \geq |\beta|, \\ 4\beta^2 & \text{if } |\alpha| \leq |\beta|. \end{cases}$$

The following lemma provides structural properties of $\overline{Q}$.

LEMMA 3.1 (convexity). *The function $\overline{Q} : \mathbb{R}^2_{\geq 0} \to \mathbb{R}$ is continuously differentiable and convex so that the mapping*

$$(z,r) \mapsto \int_0^L \overline{Q}(|z|,|r|)\,\mathrm{d}x$$

is weakly lower semicontinuous on $L^2(0,L;\mathbb{R}^3) \times L^2(0,L;\mathbb{R}^3)$.

Proof. For $\alpha \geq \beta$ we have that

$$\nabla\overline{Q}(\alpha,\beta) = \begin{bmatrix} 2\alpha - 2\beta^4/\alpha^3 \\ 4\beta + 4\beta^3/\alpha^2 \end{bmatrix},$$

and for $\alpha \leq \beta$ we have that

$$\nabla\overline{Q}(\alpha,\beta) = \begin{bmatrix} 0 \\ 8\beta \end{bmatrix},$$

so that $\overline{Q}$ is continuously differentiable. It is obvious that $D^2\overline{Q}$ is positive semidefinite if $\alpha \leq \beta$. Letting $q = \beta/\alpha$ the Hessian $D^2\overline{Q}$ for $\alpha \geq \beta$ is given by

$$D^2\overline{Q}(\alpha,\beta) = \begin{bmatrix} 2+6q^4 & -8q^3 \\ -8q^3 & 4+12q^2 \end{bmatrix}.$$

For $x = (x_1,x_2) \in \mathbb{R}^2$ we have, using $q^2 \leq 1$,

$$\begin{aligned} x^{\mathsf{T}} D^2\overline{Q}(\alpha,\beta)x &= 2x_1^2 + 4x_2^2 + q^2(6q^2x_1^2 - 16qx_1x_2 + 12x_2^2) \\ &\geq q^2(8q^2x_1^2 - 16qx_1x_2 + 16x_2^2) \geq 0, \end{aligned}$$

since, e.g., $16qx_1x_2 \leq 4q^2x_1^2 + 16x_2^2$. A Taylor expansion yields the convexity property $\overline{Q}(\widetilde{\alpha},\widetilde{\beta}) \geq \overline{Q}(\alpha,\beta) + \nabla\overline{Q}(\alpha,\beta) \cdot ((\widetilde{\alpha},\widetilde{\beta}) - (\alpha,\beta))$. ∎

3.2. Regularization. A smooth approximation of the function $\overline{Q}$ is obtained by using a regularized modulus function; i.e., we assume that for every $\delta \geq 0$ we are given a function

$$|\cdot|_\delta : \mathbb{R} \to \mathbb{R}_{\geq 0}$$

that satisfies $|\cdot|_\delta \in C^2(\mathbb{R})$, obeys the estimates

$$|\cdot|_\delta \geq c_0\delta, \quad |\cdot|'_\delta \leq c_1, \quad |\cdot|''_\delta \leq c_2\delta^{-1}, \tag{3}$$

and approximates the modulus function uniformly; i.e., for all $x \in \mathbb{R}$ we have

$$\big||x|_\delta - |x|\big| \leq c_{\mathrm{uni}}\delta. \tag{4}$$

A possible choice is the function $|x|_\delta = (x^2+\delta^2)^{1/2}$. Motivated by the relation $2\max\{x,y\} = x + y + |x-y|$, we define

$$\overline{Q}_\delta(\alpha,\beta) = 2\beta^2 + \frac{1}{2}\alpha^2 + \frac{1}{2}\beta^2 + \frac{1}{2}|\alpha^2-\beta^2|_\delta + \frac{2\beta^4}{\alpha^2+\beta^2+|\alpha^2-\beta^2|_\delta}$$

and note that $\overline{Q}_\delta$ coincides with $\overline{Q}$ for $\delta = 0$. To prove the consistency of our discretization, which will be based on the regularization, we note the following estimate.

LEMMA 3.2 (local Lipschitz continuity). *Given $\alpha, \beta, \widetilde{\alpha}, \widetilde{\beta} \in \mathbb{R}$, we have*

$$\big|\overline{Q}(\alpha,\beta) - \overline{Q}_\delta(\widetilde{\alpha},\widetilde{\beta})\big| \le 21\big(|\beta-\widetilde{\beta}||\beta+\widetilde{\beta}| + |\alpha-\widetilde{\alpha}||\alpha+\widetilde{\alpha}| + c_{\rm uni}\delta\big).$$

Proof. We define

$$s^2 = \alpha^2+\beta^2+|\alpha^2-\beta^2|, \quad \widetilde{s}^2 = \widetilde{\alpha}^2+\widetilde{\beta}^2+|\widetilde{\alpha}^2-\widetilde{\beta}^2|_\delta$$

and note that

$$\overline{Q}(\alpha,\beta) = 2\beta^2 + \frac{1}{2}s^2 + \frac{2\beta^4}{s^2}, \quad \overline{Q}_\delta(\widetilde{\alpha},\widetilde{\beta}) = 2\widetilde{\beta}^2 + \frac{1}{2}\widetilde{s}^2 + \frac{2\widetilde{\beta}^4}{\widetilde{s}^2}.$$

Straightforward calculations lead to

$$\frac{\beta^4}{s^2} - \frac{\widetilde{\beta}^4}{\widetilde{s}^2} = \frac{(\widetilde{s}^2-s^2)\beta^4}{s^2\widetilde{s}^2} + \frac{(\beta^2-\widetilde{\beta}^2)(\beta^2+\widetilde{\beta}^2)}{\widetilde{s}^2},$$

and, by exchanging the roles of the variables, in case $s^2 > 0$,

$$\frac{\widetilde{\beta}^4}{\widetilde{s}^2} - \frac{\beta^4}{s^2} = \frac{(s^2-\widetilde{s}^2)\widetilde{\beta}^4}{\widetilde{s}^2 s^2} + \frac{(\widetilde{\beta}^2-\beta^2)(\widetilde{\beta}^2+\beta^2)}{s^2}.$$

On combining the two identities, we find that

$$\Big|\frac{\beta^4}{s^2} - \frac{\widetilde{\beta}^4}{\widetilde{s}^2}\Big| \le \big(|\widetilde{s}^2-s^2| + |\beta^2-\widetilde{\beta}^2|\big)\min\Big\{\frac{\beta^4}{s^2\widetilde{s}^2} + \frac{\beta^2+\widetilde{\beta}^2}{\widetilde{s}^2}, \frac{\widetilde{\beta}^4}{s^2\widetilde{s}^2} + \frac{\beta^2+\widetilde{\beta}^2}{s^2}\Big\}.$$

Noting that $s^2 \ge \beta^2$ and $\widetilde{s}^2 \ge \widetilde{\beta}^2 + c_0\delta \ge \widetilde{\beta}^2$, the estimate implies that we have

$$\Big|\frac{\beta^4}{s^2} - \frac{\widetilde{\beta}^4}{\widetilde{s}^2}\Big| \le \big(|\widetilde{s}^2-s^2| + |\beta^2-\widetilde{\beta}^2|\big)\min\Big\{1+2\frac{\beta^2}{\widetilde{\beta}^2+c_0\delta}, 1+2\frac{\widetilde{\beta}^2}{\beta^2}\Big\}.$$

A case distinction relating β^2 and $\widetilde{\beta}^2+c_0\delta$ shows that the minimum on the right-hand side is always bounded by 3. Using (4), Lipschitz continuity of the modulus function, and binomial formulas shows that we have

$$\big|s^2-\widetilde{s}^2\big| \le 2|\alpha-\widetilde{\alpha}||\alpha+\widetilde{\alpha}| + 2|\beta-\widetilde{\beta}||\beta+\widetilde{\beta}| + c_{\rm uni}\delta.$$

Combining the estimates implies that we have

$$\begin{aligned}\big|\overline{Q}(\alpha,\beta)-\overline{Q}_\delta(\widetilde{\alpha},\widetilde{\beta})\big| &\le 2|\beta^2-\widetilde{\beta}^2| + \frac{1}{2}|s^2-\widetilde{s}^2| + 2\Big|\frac{\beta^4}{s^2} - \frac{\widetilde{\beta}^4}{\widetilde{s}^2}\Big| \\ &\le (2+6)|\beta^2-\widetilde{\beta}^2| + \Big(\frac{1}{2}+6\Big)|s^2-\widetilde{s}^2| \\ &\le |\beta-\widetilde{\beta}||\beta+\widetilde{\beta}|\big(2+6+13\big) + 13|\alpha-\widetilde{\alpha}||\alpha+\widetilde{\alpha}| + \frac{13}{2}c_{\rm uni}\delta.\end{aligned}$$

This implies the asserted estimate. ∎

3.3. Approximation. Lemma 3.2 implies the uniform convergence property $\overline{Q}_\delta \to \overline{Q}$. Another consequence is the strong approximability of the variational problem defined by E. More generally, we consider the approximation by variational problems with energy functionals E_{δ,ε_2} using the regularized function $\overline{Q}_\delta$ and a penalized treatment of the relation $y' \cdot b' = -y'' \cdot b = 0$, i.e.,

$$E_{\delta,\varepsilon_2}[y,b] = \int_0^L \overline{Q}_\delta(|y''|,|b'|)\,\mathrm{d}x + \frac{1}{2\varepsilon_2}\int_0^L (y' \cdot b')^2\,\mathrm{d}x.$$

We incorporate boundary conditions via a bounded linear operator L_{bc}, which is assumed to depend only on the boundary values of y, y', and b. It defines the set of admissible frames

$$\mathcal{A}_{\mathrm{frame}} = \big\{(y,b) \in H^2(0,L;\mathbb{R}^3) \times H^1(0,L;\mathbb{R}^3) : \\ [y', b, y' \times b] \in SO(3) \text{ a.e. in } (0,L),\ L_{\mathrm{bc}}[y,b] = \ell_{\mathrm{bc}}\big\}.$$

Note that the relation $y' \cdot b' = 0$ is not included in the set $\mathcal{A}_{\mathrm{frame}}$. The variational problem under consideration then reads as follows:

$$(\mathrm{P}_{\delta,\varepsilon_2}) \qquad \begin{cases} \text{Given } \varepsilon_2, \delta \geq 0 \text{ find a minimizing pair} \\ (y,b) \in \mathcal{A}_{\mathrm{frame}} \text{ for } E_{\delta,\varepsilon_2}[y,b]. \end{cases}$$

The original problem formally corresponds to $\delta = 0$ and $\varepsilon_2 = 0$ when the penalty term is interpreted as a strict constraint. Due to the convexity of $\overline{Q}$ a solution exists for $\delta = 0$ and $\varepsilon_2 \geq 0$. Our numerical scheme will be a discrete variant of the following approximation result, which is based on the density result of [9].

Proposition 3.3 (strong approximability). *For every $(y,b) \in \mathcal{A}_{\mathrm{frame}}$ with $y' \cdot b' = 0$ and every $\sigma > 0$ there exists*

$$(y_\sigma, b_\sigma) \in \big[C^\infty(0,L;\mathbb{R}^3)\big]^2 \cap \mathcal{A}_{\mathrm{frame}}$$

with $y_\sigma' \cdot b_\sigma' = 0$,

$$\|y - y_\sigma\|_{H^2(0,L)} + \|b - b_\sigma\|_{H^1(0,L)} \leq \sigma,$$

such that

$$\big|E[y,b] - E_{\delta,\varepsilon_2}[y_\sigma, b_\sigma]\big| \leq c_{\mathrm{sa}}(\delta + \sigma).$$

In particular, the functionals $\big(E_{\delta,\varepsilon_2}\big)_{\delta,\varepsilon_2}$ are Γ-convergent to E for $(\delta,\varepsilon_2) \to 0$.

Proof. The results from [9, Theorem 4.1] provide the pairs $(y_\sigma, b_\sigma) \in \mathcal{A}_{\mathrm{frame}}$ for every $\sigma > 0$ with the structural property $y_\sigma' \cdot b_\sigma' = 0$. The Γ convergence result is an immediate consequence of the estimates. ∎

Remark 3.4. We remark that the quantity

$$[y,b]_\sigma = \|y_\sigma\|_{H^3(0,L)} + \|b_\sigma\|_{H^2(0,L)}$$

is in general unbounded as $\sigma \to 0$. If $(y,b) \in H^3(0,L;\mathbb{R}^3) \times H^2(0,L;\mathbb{R}^3)$, then it remains bounded.

4. Finite element approximation. We write the regularized minimization problem with a penalized treatment of the orthogonality relations as

$$\begin{aligned} E_{\delta,\varepsilon}[y,b] &= \int_0^L \overline{Q}_\delta(|y''|,|b'|)\,\mathrm{d}x + P_\varepsilon[y,b] \\ &= \frac{1}{2}\int_0^L |y''|^2 + 5|b'|^2 + \psi_\delta(|y''|^2,|b'|^2)\,\mathrm{d}x + P_\varepsilon[y,b], \end{aligned}$$

where for $\varepsilon = (\varepsilon_1,\varepsilon_2)$ we define

$$P_\varepsilon[y,b] = \frac{1}{2\varepsilon_1}\int_0^L (y'\cdot b)^2\,\mathrm{d}x + \frac{1}{2\varepsilon_2}\int_0^L (y'\cdot b')^2\,\mathrm{d}x,$$

and the function ψ_δ is defined via

$$\psi_\delta(\alpha^2,\beta^2) = |\alpha^2-\beta^2|_\delta + \frac{4\beta^4}{\alpha^2+\beta^2+|\alpha^2-\beta^2|_\delta}.$$

The minimization of $E_{\delta,\varepsilon}$ is subject to the pointwise unit length conditions

$$|y'|^2 = 1, \quad |b|^2 = 1.$$

The corresponding discrete problem uses subspaces $V_h \subset V$ with

$$\begin{aligned} V_h &= \mathcal{S}^{3,1}(\mathcal{T}_h)^3 \times \mathcal{S}^{1,0}(\mathcal{T}_h)^3, \\ V &= H^2(0,L;\mathbb{R}^3)\times H^1(0,L;\mathbb{R}^3). \end{aligned}$$

By imposing the nonlinear constraints at the nodes of the partitioning $\mathcal{T}_h$, we arrive at the following discrete problem.

$$(\mathrm{P}_{\delta,\varepsilon,h}) \qquad \begin{cases} \text{Find a minimizing pair } (y_h,b_h)\in V_h \text{ for} \\ E_{\delta,\varepsilon,h}[y_h,b_h] = \dfrac{1}{2}\displaystyle\int_0^L |y_h''|^2 + 5|b_h'|^2 + \psi_\delta(|y_h''|^2,|b_h'|^2)\,\mathrm{d}x \\ \qquad\qquad\qquad\qquad + P_\varepsilon[y_h,b_h] \\ \text{subject to} \quad \mathcal{I}_h^{1,0}|y_h'|^2 = \mathcal{I}_h^{1,0}|b_h|^2 = 1 \text{ and } L_{\mathrm{bc}}[y_h,b_h] = \ell_{\mathrm{bc}}. \end{cases}$$

The following proposition implies that discrete minimizers converge to minimizers of the continuous problem. Because of the assumption that the operator L_{bc} only depends on the boundary values of y, y', and b, these are preserved under the nodal interpolation operators $\mathcal{I}_h^{3,1}$ and $\mathcal{I}_h^{1,0}$.

PROPOSITION 4.1 (Γ convergence). *The discrete constrained energy functionals $E_{\varepsilon,\delta,h}$ approximate the continuous constrained energy functional E in the sense of the following assertions.*

(i) *Let $(y,b)\in V$. If $(\varepsilon_1,\varepsilon_2,\delta)\to 0$ such that*

$$h^2\varepsilon_1^{-1} + h^2\varepsilon_2^{-1} = o(1)$$

as $h\to 0$, then there exists a sequence of discrete admissible pairs $(y_h,b_h)\in V_h$ with $y_h\to y$ in H^2 and $b_h\to b$ in H^1 as $h\to 0$ and such that

$$E_{\delta,\varepsilon,h}[y_h,b_h]\to E[y,b].$$

(ii) *For every bounded sequence $(y_h, b_h) \in V_h$ of admissible pairs with weak limit $(y, b) \in V$ we have that the limiting pair is admissible and that*

$$E[y, b] \leq \liminf_{(\varepsilon,\delta,h)\to 0} E_{\delta,\varepsilon,h}[y_h, b_h].$$

Proof. (i) We use the result of Proposition 3.3 and consider for $\sigma > 0$ the smooth frame $(y_\sigma, b_\sigma) \in \mathcal{A}_{\text{frame}}$ that approximates the general frame $(y, b) \in \mathcal{A}_{\text{frame}}$. We then consider for $h > 0$ the pair (y_h, b_h) defined via

$$y_h = \mathcal{I}_h^{3,1} y_\sigma, \quad b_h = \mathcal{I}_h^{1,0} b_\sigma.$$

We have that $(y_h, b_h) \to (y, b)$ in $H^2(0, L; \mathbb{R}^3) \times H^1(0, L; \mathbb{R}^3)$. Moreover, the pair (y_h, b_h) is admissible in the discrete minimization problem; i.e., the functions satisfy the boundary conditions and the nodal unit length constraints. Since $y_\sigma' \cdot b_\sigma = 0$, we find that

$$y_h' \cdot b_h = (y_h' - y_\sigma') \cdot b_h + y_\sigma' \cdot (b_h - b_\sigma),$$

and hence we have

$$\|y_h' \cdot b_h\| \leq ch.$$

Similarly, with the quantity $c_\sigma = [y, b]_\sigma$ from Remark 3.4 that bounds the norms $\|y_\sigma\|_{H^3(0,L)}$ and $\|b_\sigma\|_{H^2(0,L)}$, we have that

$$\|y_h' \cdot b_h'\| \leq chc_\sigma.$$

The repeated application of Lemma 3.2 provides the estimate

$$\begin{aligned}\big|\overline{Q}_\delta(\alpha, \beta) - \overline{Q}_\delta(\widetilde{a}, \widetilde{b})\big| &\leq \big|\overline{Q}_\delta(\alpha, \beta) - \overline{Q}(\alpha, \beta)\big| + \big|\overline{Q}(\alpha, \beta) - \overline{Q}_\delta(\widetilde{a}, \widetilde{b})\big| \\ &\leq c\big(|\beta - \widetilde{\beta}||\beta + \widetilde{\beta}| + |\alpha - \widetilde{\alpha}||\alpha + \widetilde{\alpha}| + \delta\big).\end{aligned}$$

In combination with Proposition 3.3 this yields that

$$\begin{aligned}&\big|E[y, b] - E_{\delta,\varepsilon,h}[y_h, b_h]\big| \\ &\qquad \leq \big|E[y, b] - E_{\delta,\varepsilon_2}[y_\sigma, b_\sigma]\big| + \big|E_{\delta,\varepsilon_2}[y_\sigma, b_\sigma] - E_{\delta,\varepsilon,h}[y_h, b_h]\big| \\ &\qquad \leq c\big(\delta + \sigma\big) + c\big(hc_\sigma + \delta + h^2\varepsilon_1^{-1} + (h^2 c_\sigma^2)\varepsilon_2^{-1}\big).\end{aligned}$$

The conditions of the proposition imply that the right-hand side tends to zero as $h \to 0$.

(ii) Assume that $(y_h, b_h)_{h>0}$ is a sequence of admissible discrete pairs with weak limit $(y, b) \in V$. We may assume that the sequence $E_{\delta,\varepsilon,h}[y_h, b_h]$ is bounded. Compactness properties of embeddings imply that $|y'|^2 = 1$ and $|b|^2 = 1$ in $(0, L)$. Since $P_\varepsilon[y_h, b_h]$ is bounded, we have that $y_h' \cdot b_h$ and $y_h' \cdot b_h'$ converge to zero in $L^2(0, L)$. Noting that $y_h' \to y'$ in $L^\infty(0, L; \mathbb{R}^3)$ it follows that $y' \cdot b = 0$ and $y' \cdot b' = 0$. Since L_{bc} is bounded and linear, it is weakly continuous, and we verify that $L_{\text{bc}}[y, b] = \ell_{\text{bc}}$. Hence, we conclude that $(y, b) \in \mathcal{A}_{\text{frame}}$. Since the functional E is weakly lower semicontinuous, since the functionals P_ε are nonnegative, and since the regularization of the integrand $\overline{Q}$ is uniformly controlled by Lemma 3.2, we find that

$$\begin{aligned}E[y, b] &\leq \liminf_{h\to 0} E[y_h, b_h] \\ &\leq \liminf_{(\varepsilon,h,\delta)\to 0} E_{\delta,\varepsilon,h}[y_h, b_h] + c\delta \\ &= \liminf_{(\varepsilon,h,\delta)\to 0} E_{\delta,\varepsilon,h}[y_h, b_h].\end{aligned}$$

This proves the proposition. ∎

Remark 4.2. The conditions of the proposition are satisfied if $\varepsilon_1 = \varepsilon_2 = h^\beta$, $j = 1, 2$, with $\beta < 2$. If $y \in H^3(0, L; \mathbb{R}^3)$ and $b \in H^2(0, L; \mathbb{R}^3)$, then we may choose $\beta = 2$.

The numerical realization of the functionals $E_{\delta,\varepsilon,h}$ requires the use of quadrature. For an element $T = [x_1, x_2]$ and a function $v \in C(T)$ we use averaging operators defined via

$$\mathcal{A}_h v|_T = |T|^{-1} \int_T v \,\mathrm{d}x, \quad \mathcal{M}_h v|_T = |T|^{-1} \int_T \mathcal{I}_h^{1,0} v \,\mathrm{d}x.$$

For $r \in C^1(T)$ we have that

$$\mathcal{A}_h r'|_T = h_T^{-1}\big(r(x_2) - r(x_1)\big), \quad \mathcal{M}_h r|_T = \frac{1}{2}\big(r(x_1) + r(x_2)\big).$$

The operator $\mathcal{A}_h : L^2(0, L) \to L^2(0, L)$ is bounded and self-adjoint; as a consequence of Jensen's or Hölder's inequality we have

$$\|\mathcal{A}_h y_h''\| \le \|y_h''\|. \tag{5}$$

Moreover, we have the estimates

$$\|y_h' - \mathcal{M}_h y_h'\|_{L^\infty(0,L)} \le c h^{1/2} \|y_h''\|,$$
$$\|\mathcal{A}_h y_h'' - y_h''\| \le c h \|y_h'''\|.$$

With the help of the operators $\mathcal{A}_h$ and $\mathcal{M}_h$ we define a discrete functional which allows for exact numerical integration and which Γ-converges to the continuous variational problem under different conditions on the parameters.

Proposition 4.3 (quadrature). *The result of Proposition* 4.1 *remains valid if* $E_{\delta,\varepsilon,h}$ *is replaced by the functional*

$$E^{\mathrm{quad}}_{\delta,\varepsilon,h}[y_h, b_h] = \frac{1}{2}\int_0^L |y_h''|^2 + 5|b_h'|^2 + \psi_\delta(|\mathcal{A}_h y_h''|^2, |b_h'|^2)\,\mathrm{d}x$$
$$+ \frac{1}{2\varepsilon_1}\int_0^L \mathcal{I}_h^{1,0}\big[(y_h' \cdot b_h)^2\big]\,\mathrm{d}x + \frac{1}{2\varepsilon_2}\int_0^L (\mathcal{M}_h y_h' \cdot b_h')^2\,\mathrm{d}x;$$

i.e., it approximates E *in the sense of Proposition* 4.1 *if the condition* $h^2\varepsilon_1^{-1} + h^2\varepsilon_2^{-1} = o(1)$ *is replaced by* $h^{1/2}\varepsilon_2^{-1} \to 0$ *as* $h \to 0$.

Proof. We discuss necessary changes in the proof of Proposition 4.1.

If the sequence $(y_h, b_h)_{h>0}$ is obtained by interpolating a regular sequence of frames, we have that $y_h' \cdot b_h$ vanishes at the nodes so that $\mathcal{I}_h[(y_h' \cdot b_h)] = 0$ and the first penalty term in $E^{\mathrm{quad}}_{\delta,\varepsilon,h}[y_h, b_h]$ vanishes. For a sequence (y_h, b_h) with bounded energies we have $\|\mathcal{I}_h[(y_h' \cdot b_h)^2]\|_{L^1(0,L)} \le c\varepsilon_1$, which implies that $y' \cdot b = 0$ for accumulation points. For the second penalty term we have for a bounded sequence $(y_h, b_h)_{h>0}$ in $H^2(0, L; \mathbb{R}^3) \times H^1(0, L; \mathbb{R}^3)$ that

$$\Big|\frac{1}{\varepsilon_2}\int_0^L (\mathcal{M}_h y_h' \cdot b_h')^2 - (y_h' \cdot b_h')^2\,\mathrm{d}x\Big|$$
$$\le \varepsilon_2^{-1}\|\mathcal{M}_h y_h' - y_h'\|_{L^\infty(0,L)}\|b_h'\|^2\|\mathcal{M}_h y_h' + y_h'\|_{L^\infty(0,L)} \le c h^{1/2}\varepsilon_2^{-1}.$$

(i) For the attainment result we note that the Lipschitz continuity of ψ_δ (see Lemma 5.2 below) yields the estimate

$$\begin{aligned}\int_0^L \Big|\psi_\delta(|\mathcal{A}_h y_h''|^2, |b_h'|^2) - \psi_\delta(|y_h''|^2, |b_h'|^2)\Big| \,\mathrm{d}x \\ \le c_\psi \int_0^L |\mathcal{A}_h y_h'' - y_h''||\mathcal{A}_h y_h'' + y_h''| \,\mathrm{d}x \le ch\|y_h'''\| \le chc_\sigma,\end{aligned}$$

where we used that the interpolation operator $\mathcal{I}_h^{3,1}$ is elementwise stable in H^3. Hence, we have that

$$\lim_{(h,\delta)\to 0} E^{\mathrm{quad}}_{\delta,\varepsilon,h}[y_h, b_h] = E[y, b].$$

(ii) To establish the lower bound property, we note that if $y_h \rightharpoonup y$ in $H^2(0, L; \mathbb{R}^3)$ and $b_h \rightharpoonup b$ in $H^1(0, L; \mathbb{R}^3)$, then (5) and the weak lower semicontinuity of E identified in Lemma 3.1 show that

$$\begin{aligned}\liminf_{h,\delta\to 0} \frac{1}{2}\int_0^L |y_h''|^2 + 5|b_h'|^2 + \psi_\delta(|\mathcal{A}_h y_h''|^2, |b_h'|^2) \,\mathrm{d}x \\ \ge \liminf_{h,\delta\to 0} \int_0^L |\mathcal{A}_h y_h''|^2 + 5|b_h'|^2 + \psi_\delta(|\mathcal{A}_h y_h''|^2, |b_h'|^2) \,\mathrm{d}x \\ \ge \liminf_{h,\delta\to 0} \int_0^L |\mathcal{A}_h y_h''|^2 + 5|b_h'|^2 + \psi(|\mathcal{A}_h y_h''|^2, |b_h'|^2) \,\mathrm{d}x - c\delta \\ = \liminf_{h\to 0} \int_0^L \overline{Q}(|\mathcal{A}_h y_h''|, |b_h'|) \,\mathrm{d}x \\ \ge \int_0^L |y''|^2 + 5|b'|^2 + \psi(|y''|^2, |b'|^2) \,\mathrm{d}x.\end{aligned}$$

This implies that $E[y, b] \le \liminf_{(\varepsilon,\delta,h)\to 0} E^{\mathrm{quad}}_{\delta,\varepsilon,h}[y_h, b_h]$ and proves the assertion. ∎

Remark 4.4. To approximate regular minimizers, e.g., satisfying the condition $y \in W^{2,\infty}(0, L; \mathbb{R}^3)$, it suffices to impose the condition $h\varepsilon_2^{-1} \to 0$.

5. Iterative minimization.

5.1. Discrete gradient flow. We devise a decoupled gradient scheme with a linearized treatment of the pointwise constraints to compute stationary configurations. For ease of readability we often omit the spatial discretization parameter h in what follows and denote

$$Y_h = \mathcal{S}^{3,1}(\mathcal{T}_h)^3, \quad B_h = \mathcal{S}^{1,0}(\mathcal{T}_h)^3.$$

The variational derivatives of the (discretized) penalty functional $P_{\varepsilon,h}$ with respect to y and b are denoted by $\delta_y P_\varepsilon$ and $\delta_b P_\varepsilon$, respectively. For the function ψ_δ the partial derivatives are denoted by $\psi'_{\delta,1}$ and $\psi'_{\delta,2}$. We assume that the boundary conditions are separated, i.e., that we have

$$L_{\mathrm{bc}}[y, b] = \big(L^1_{\mathrm{bc}}[y], L^2_{\mathrm{bc}}[b]\big),$$

and $\ell_{\mathrm{bc}} = (\ell^1_{\mathrm{bc}}, \ell^2_{\mathrm{bc}})$.

ALGORITHM 5.1 (gradient descent). *Choose* $\tau > 0$ *and* $(y_0, b_0) \in Y_h \times B_h$ *with*

$$L^1_{\mathrm{bc}}[y_0] = \ell^1_{\mathrm{bc}}, \quad L^2_{\mathrm{bc}}[b_0] = \ell^2_{\mathrm{bc}},$$

and the nodal length conditions

$$|y_0'|^2 = 1, \quad |b_0|^2 = 1;$$

set $k = 1$.

(1) *Compute* $y_k \in Y_h$ *such that*

$$(d_t y_k, w)_\star + (y_k'', w'') + \delta_y P_\varepsilon[y_k, b_{k-1}; w] \\ = -(\psi_{\delta,1}'(|\mathcal{A} y_{k-1}''|^2, |b_{k-1}'|^2)\mathcal{A} y_{k-1}'', \mathcal{A} w'')$$

for all $w \in Y_h$ *subject to the nodal constraints*

$$d_t y_k' \cdot y_{k-1}' = 0, \quad w' \cdot y_{k-1}' = 0$$

and the boundary conditions

$$L^1_{\mathrm{bc}}[d_t y_k] = 0, \quad L^1_{\mathrm{bc}}[w] = 0.$$

(2) *Compute* $b_k \in B_h$ *such that*

$$(d_t b_k, r)_\dagger + 5(b_k', r') + \delta_b P_\varepsilon[y_k, b_k; r] \\ = -(\psi_{\delta,2}'(|\mathcal{A} y_{k-1}''|^2, |b_{k-1}'|^2) b_{k-1}', r')$$

for all $r \in B_h$ *subject to the nodal constraints*

$$d_t b_k \cdot b_{k-1} = 0, \quad r \cdot b_{k-1} = 0$$

and the boundary conditions

$$L^2_{\mathrm{bc}}[d_t b_k] = 0, \quad L^2_{\mathrm{bc}}[r] = 0.$$

(3) *Stop the iteration if* $\|d_t y_k\|_\star + \|d_t b_k\|_\dagger \le \varepsilon_{\mathrm{stop}}$*; set* $k \to k+1$*, and continue with* (1) *otherwise.*

We remark that all steps of Algorithm 5.1 define linear systems of equations that can be solved efficiently.

5.2. Linearization estimates. The iterative numerical treatment of the model problem requires the use of linearizations of nonlinearities occurring in the energy functional. The following lemmas provide estimates on derivatives of the nonquadratic part of the regularized function $\overline{Q}_\delta$.

LEMMA 5.2 (derivative bounds). *The function* ψ_δ*, for* $r, s \in \mathbb{R}_{\ge 0}$ *defined via*

$$\psi_\delta(r,s) = |r-s|_\delta + \frac{4s^2}{r+s+|r-s|_\delta},$$

satisfies

$$|\nabla \psi_\delta| \le c_{\psi,1}, \quad |D^2 \psi_\delta| \le c_{\psi,2} \delta^{-1}.$$

Proof. Let $\sigma_\delta = |\cdot|_\delta'$ and $D_\delta = \sigma_\delta' = |\cdot|_\delta''$. We have

$$\partial_1 \psi_\delta(r,s) = \sigma_\delta(r-s) - \frac{4s^2}{(r+s+|r-s|_\delta)^2}(1+\sigma_\delta(r-s)),$$

$$\partial_2 \psi_\delta(r,s) = -\sigma_\delta(r-s) + \frac{8s}{r+s+|r-s|_\delta} - \frac{4s^2}{(r+s+|r-s|_\delta)^2}(1-\sigma_\delta(r-s)).$$

The formulas imply the uniform boundedness of the partial derivatives. For higher order partial derivatives we have, e.g.,

$$\partial_1^2\psi_\delta(r,s) = D_\delta(r-s) + \frac{8s^2}{(r+s+|r-s|_\delta)^3}\big(1+\sigma_\delta(r-s)\big)^2 - \frac{4s^2}{(r+s+|r-s|_\delta)^2}D_\delta(r-s).$$

The remaining second order derivatives lead to similar formulas. Incorporating the assumptions on the second derivative of the regularized modulus function and using a case distinction relating $r+s$ to δ imply the bounds on the Hessian of ψ_δ. ∎

A Taylor formula is needed to control the explicit treatment of the nonlinear part ψ_δ in Algorithm 5.1.

LEMMA 5.3 (Taylor formula). *For all $a,b,\widetilde{a},\widetilde{b}\in\mathbb{R}^3$ there exist $\widehat{a},\widehat{b}\in\mathbb{R}^3$ such that*

$$\frac{1}{2}\big(\psi_\delta(|a|^2,|b|^2)-\psi_\delta(|\widetilde{a}|^2,|\widetilde{b}|^2)\big) - \nabla\psi_\delta(|\widetilde{a}|^2,|\widetilde{b}|^2)\cdot\begin{bmatrix}\widetilde{a}\cdot(a-\widetilde{a})\\ \widetilde{b}\cdot(b-\widetilde{b})\end{bmatrix} = \Gamma(\widehat{a},\widehat{b},a,b,\widetilde{a},\widetilde{b}),$$

with a function Γ that satisfies

$$\big|\Gamma(\widehat{a},\widehat{b},a,b,\widetilde{a},\widetilde{b})\big| \le c_\Gamma\big[\delta^{-1}\big(|a|^2+|\widetilde{a}|^2+|b|^2+|\widetilde{b}|^2\big)+1\big]\big(|a-\widetilde{a}|^2+|b-\widetilde{b}|^2\big).$$

Proof. Defining $g(a,b)=(1/2)\psi_\delta(|a|^2,|b|^2)$, we have

$$g(a,b)-g(\widetilde{a},\widetilde{b})-Dg(\widetilde{a},\widetilde{b})\begin{bmatrix}a-\widetilde{a}\\ b-\widetilde{b}\end{bmatrix} = \frac{1}{2}\begin{bmatrix}a-\widetilde{a}\\ b-\widetilde{b}\end{bmatrix}^{\mathsf{T}} D^2g(\widehat{a},\widehat{b})\begin{bmatrix}a-\widetilde{a}\\ b-\widetilde{b}\end{bmatrix},$$

where $(\widehat{a},\widehat{b})$ belongs to the line segment connecting (a,b) with $(\widetilde{a},\widetilde{b})$. We have

$$\partial_1 g(\widehat{a},\widehat{b}) = \partial_1\psi_\delta(|\widehat{a}|^2,|\widehat{b}|^2)\widehat{a},\quad \partial_2 g(\widehat{a},\widehat{b}) = \partial_2\psi_\delta(|\widehat{a}|^2,|\widehat{b}|^2)\widehat{b},$$

and, consequently,

$$\begin{aligned}\partial_1^2 g(\widehat{a},\widehat{b}) &= 2\partial_1^2\psi_\delta(|\widehat{a}|^2,|\widehat{b}|^2)\widehat{a}\widehat{a}^{\mathsf{T}} + \partial_1\psi_\delta(|\widehat{a}|^2,|\widehat{b}|^2)I_{3\times3},\\ \partial_2^2 g(\widehat{a},\widehat{b}) &= 2\partial_2^2\psi_\delta(|\widehat{a}|^2,|\widehat{b}|^2)\widehat{b}\widehat{b}^{\mathsf{T}} + \partial_2\psi_\delta(|\widehat{a}|^2,|\widehat{b}|^2)I_{3\times3},\\ \partial_1\partial_2 g(\widehat{a},\widehat{b}) &= 2\partial_1\partial_2\psi_\delta(|\widehat{a}|^2,|\widehat{b}|^2)\widehat{b}\,\widehat{a}^{\mathsf{T}}.\end{aligned}$$

The bounds of Lemma 5.2 imply the asserted result. ∎

5.3. Energy monotonicity. Stability of Algorithm 5.1 can be established if the step size τ satisfies a smallness condition defined by the regularization parameter δ and the mesh-size h. The following proposition implies that the iteration approximates stationary points for the discrete energy functional.

PROPOSITION 5.4 (energy decay). *Assume that there exist $c_\star, c_\dagger > 0$ such that for all $w\in Y_h$ and $r\in B_h$ we have*

$$\|w\|_{H^2(0,L)} \le c_\star\|w\|_\star,\quad \|r\|_{H^1(0,L)} \le c_\dagger\|r\|_\dagger.$$

Then there exists a constant $c_{\rm ed} > 0$ *such that for the uniquely defined iterates* $(y_k, b_k)_{k=0,1,\dots}$ *of Algorithm* 5.1 *we have*

$$E_{\delta,\varepsilon,h}[y_K, b_K] + \big(1 - c_{\rm ed}\tau\delta^{-1}h^{-1}\big)\tau\sum_{k=1}^{K}\big(\|d_t y_k\|_\star^2 + \|d_t b_k\|_\dagger^2\big) \le E_{\delta,\varepsilon,h}[y_0, b_0].$$

Moreover, if $2c_{\rm ed}\tau \le \delta h$, *we have that*

$$\|\mathcal{I}_h^{1,0}|b_k|^2 - 1\|_{L^\infty(0,L)} + \|\mathcal{I}_h^{1,0}|y_k'|^2 - 1\|_{L^\infty(0,L)} \le c_{\rm ul}\tau e_0,$$

with $e_0 = E_{\delta,\varepsilon,h}[y_0, b_0]$.

Proof. We adopt an inductive argument and first prove an intermediate bound, which will allow us to control the explicit treatment of the nonlinearities related to ψ. The conditional energy decay estimate then implies the control of the violation of the pointwise constraints. Well-posedness of the iteration is an immediate consequence of the Lax–Milgram lemma.

Step 1. We choose $w = d_t y_k$ and $r = d_t b_k$ in Steps (1) and (2) of Algorithm 5.1. Using (2) and incorporating (5) this implies that

$$\begin{aligned}(6)\quad &\|d_t y_k\|_\star^2 + \|d_t b_k\|_\dagger^2 + d_t\Big(\frac{1}{2}\|y_k''\|^2 + \frac{5}{2}\|b_k'\|^2 + P_{\varepsilon,h}[y_k, b_k]\Big)\\ &\qquad \le \|\nabla\psi_\delta(|\mathcal{A}y_{k-1}''|^2, |b_{k-1}'|^2)\|_{L^\infty(0,L)}\big(\|y_{k-1}''\|\|d_t y_k''\| + \|b_{k-1}'\|\|d_t b_k'\|\big).\end{aligned}$$

Here, we used that the separate convexity of $P_{\varepsilon,h}$ implies that we have

$$P_{\varepsilon,h}[y_k, b_{k-1}] + \delta_y P_{\varepsilon,h}[y_k, b_{k-1}; y_{k-1} - y_k] \le P_{\varepsilon,h}[y_{k-1}, b_{k-1}]$$

and

$$P_{\varepsilon,h}[y_k, b_k] + \delta_b P_{\varepsilon,h}[y_k, b_k; b_{k-1} - b_k] \le P_{\varepsilon,h}[y_k, b_{k-1}],$$

which by summation and multiplication by $1/\tau$ yields that

$$\begin{aligned}d_t P_{\varepsilon,h}[y_k, b_k] &= \frac{1}{\tau}\big(P_{\varepsilon,h}[y_k, b_k] - P_{\varepsilon,h}[y_{k-1}, b_{k-1}]\big)\\ &\le \delta_y P_{\varepsilon,h}[y_k, b_{k-1}; d_t y_k] + \delta_b P_{\varepsilon,h}[y_k, b_k; d_t b_k].\end{aligned}$$

In an inductive argument we assume that $E_{\delta,\varepsilon}[y_{k-1}, b_{k-1}] \le e_0$, which yields

$$\frac{1}{2}\|y_{k-1}''\|^2 + \frac{5}{2}\|b_{k-1}'\|^2 + P_{\varepsilon,h}[y_{k-1}, b_{k-1}] \le e_0.$$

With (6) and Lemma 5.2 we find that

$$\begin{aligned}&\tau\Big(\frac{1}{2}\|d_t y_k\|_\star^2 + \frac{1}{2}\|d_t b_k\|_\dagger^2\Big) + \Big(\frac{1}{2}\|y_k''\|^2 + \frac{5}{2}\|b_k'\|^2 + P_{\varepsilon,h}[y_k, b_k]\Big)\\ &\qquad \le e_0 + \tau\frac{c_{\psi,1}^2}{2}\max\{c_\star^2, c_\dagger^2\}\big(\|y_{k-1}''\|^2 + \|b_{k-1}'\|^2\big)\\ &\qquad \le e_0 + \tau\frac{c_{\psi,1}^2}{2}\max\{c_\star^2, c_\dagger^2\}2e_0 = (1 + \tau C_0)e_0 \le 2e_0,\end{aligned}$$

where we assumed that $\tau C_0 \le 1$. The next step shows that $E_{\delta,\varepsilon,h}[y^k, b^k] \le e_0$ and hence implies that the right-hand side can be replaced by e_0.

Step 2. We again choose $w = d_t y_k$ and $r = d_t b_k$ in Steps (1) and (2) of Algorithm 5.1 but use the Taylor formula of Lemma 5.3 to verify that

$$d_t\Big(\frac{1}{2}\|y_k''\|^2 + \frac{5}{2}\|b_k'\|^2 + \int_0^L \psi_\delta(|\mathcal{A}y_k''|^2, |b_k'|^2)\,\mathrm{d}x + P_{\varepsilon,h}[y_k, b_k]\Big) + \|d_t y_k\|_\star^2 + \|d_t b_k\|_\dagger^2 \le \tau^{-1}\int_0^L \Gamma(\mathcal{A}\widehat{y}_k'', \widehat{b}_k', \mathcal{A}y_{k-1}'', b_{k-1}', \mathcal{A}y_k'', b_k')\,\mathrm{d}x,$$

where, using that $\|\mathcal{A}r\|_{L^\infty(0,L)} \le \|r\|_{L^\infty(0,L)}$,

$$\tau^{-1}\int_0^L \Gamma(\mathcal{A}\widehat{y}_k'', \widehat{b}_k', \mathcal{A}y_{k-1}'', b_{k-1}', \mathcal{A}y_k'', b_k')\,\mathrm{d}x \le c_\Gamma\tau\delta^{-1}\big(\|y_k''\|_{L^\infty(0,L)}^2 + \|y_{k-1}''\|_{L^\infty(0,L)}^2 + \|b_k'\|_{L^\infty(0,L)}^2 + \|b_{k-1}'\|_{L^\infty(0,L)}^2 + 1\big) \times \big(\|d_t y_k''\|^2 + \|d_t b_k'\|^2\big).$$

Using the available bounds and the inverse estimate (1), we deduce that

$$\int_0^L \Gamma(\dots)\,\mathrm{d}x \le c_\Gamma\tau\delta^{-1}\big(4c_{\mathrm{inv}}h^{-1}8e_0 + 1\big)\max\{c_\star^2, c_\dagger^2\}\big(\|d_t y_k\|_\star^2 + \|d_t b_k\|_\dagger^2\big).$$

This implies that we have

$$d_t E_{\delta,\varepsilon}[y_k, b_k] + \big(1 - c_{\mathrm{ed}}\tau\delta^{-1}h^{-1}\big)\big(\|d_t y_k\|_\star^2 + \|d_t b_k\|_\dagger^2\big) \le 0.$$

A summation over $k = 1, 2, \dots, K$ and multiplication by τ yield the energy estimate for some K, which implies the induction hypothesis.

Step 3. To derive the bounds that control the violation of the constraints we note that at the nodes we have

$$|b_k|^2 = |b_{k-1}|^2 + \tau^2|d_t b_k|^2 = \cdots = |b_0|^2 + \tau^2\sum_{r=1}^{k}|d_t b_r|^2.$$

Incorporating the identity $|b_0|^2 = 1$ and taking the L^∞ norm imply the constraint violation estimate. The same argument applies to $|y_k'|^2$. ∎

6. Numerical experiments.

6.1. Realization. With the quadrature introduced in Proposition 4.3, Algorithm 5.1 can be realized exactly and only requires solving linear systems of equations. These define certain linear saddle-point problems with unique solutions. We always use the inner products related to the norms

$$\|w\|_\star^2 = \|w\|^2 + \|w''\|^2, \quad \|r\|_\dagger^2 = \|r\|^2 + \|r'\|^2$$

and the relations

$$\tau = h/10, \quad \varepsilon_1 = h, \quad \varepsilon_2 = h^{1/2}, \quad \delta = h^{1/2}.$$

In view of Proposition 5.4, this choice for τ may be too optimistic in general. However, we always observed energy monotonicity in our experiments, which may be related to an additional regularity property. We confirm our theoretical findings by showing that our numerical scheme reliably and efficiently detects stationary configurations

of low energy via discrete evolutions from given initial states. In what follows we visualize the ribbon by introducing an artificial positive width. In addition to the discretized dimensionally reduced elastic energy $E_{\delta,\varepsilon,h}$ and the penalty term $P_{\varepsilon,h}$, we also investigate the behavior of the bending and twist energies given by

$$E_{\mathrm{bend}}[y] = \frac{1}{2}\int_0^L |y''|^2 \,\mathrm{d}x, \quad E_{\mathrm{twist}}[b] = \frac{1}{2}\int_0^L |b'|^2 \,\mathrm{d}x.$$

We always consider clamped boundary conditions for the deformation y and Dirichlet boundary conditions for the director b, which are specified via the initial states; i.e., we impose

$$y(x) = y_0(x), \quad y'(x) = y_0'(x), \quad b(x) = b_0(x)$$

at the endpoints $x \in \{0, L\}$. To satisfy the condition $y_0' \cdot b_0 = 0$ the vector field b_0 is obtained by rotating a nontangential vector field n_0 around the tangent vector y_0'. The condition $y_0' \cdot b_0' = 0$ is not taken into account in the construction of b_0 but will be approximated via the involved penalization. The discrete initial states are defined via nodal interpolation of the continuous initial states, i.e.,

$$y_h^0 = \mathcal{I}_h^{3,1} y_0, \quad b_h^0 = \mathcal{I}_h^{1,0} b_0.$$

All computations are carried out on triangulations that are given by uniform partitions of the intervals $(0, L)$ into N subintervals of length $h = L/N$. We occasionally refer to the quantities $|y_h''|$ and $|b_h'|$ as curvature and torsion of a ribbon. We always ran the discrete gradient flow with fixed time horizons $T = 6$ and $T = 10$.

6.2. Möbius ribbon. We consider boundary conditions that lead to the formation of a Möbius strip of small, vanishing width. The energy minimization reduces the elastic energy among all possible topological Möbius strips. Analytical properties of Möbius strips in the case of small positive widths are discussed in [6, 14]. The following example defines a twisted frame for the unit circle which will deform into a stationary configuration for the reduced elastic energy.

Example 6.1 (Möbius ribbon). Set $L = 2\pi$, and define for $x \in (0, L)$

$$y_0(x) = \big(\cos(x), \sin(x), 0\big)$$

and with $\alpha = 1/2$

$$b_0 = \cos(\alpha\cdot)(y_0' \times n_0) \times y_0' + \sin(\alpha\cdot) y_0' \times n_0,$$

with $n_0 = [y_0']_2^\perp$ being the rotation of the first two components of y_0' by $\pi/2$, i.e., $[a]_2^\perp = (-a_2, a_1, 0)$ for $a \in \mathbb{R}^3$.

Figure 1 shows snapshots of the discrete evolution defined by Algorithm 5.1 in Example 6.1 for a partitioning of $(0, L)$ into $N = 320$ intervals. We observe an immediate change in shape of the ribbon towards a Möbius strip. The initially constant curvature becomes nonconstant and appears to vanish in neighborhoods of three points in the nearly stationary configuration. This effect can also be seen in Figure 2, where the stationary state is visualized from two other perspectives. In points where curvature vanishes, the original Sadowsky functional is singular, and the correction from [6] becomes particularly relevant. The pure bending energy defined by the deformation of the centerline increases during the discrete gradient flow evolution, while the twist energy and the dimensionally reduced energy decay monotonically and quickly

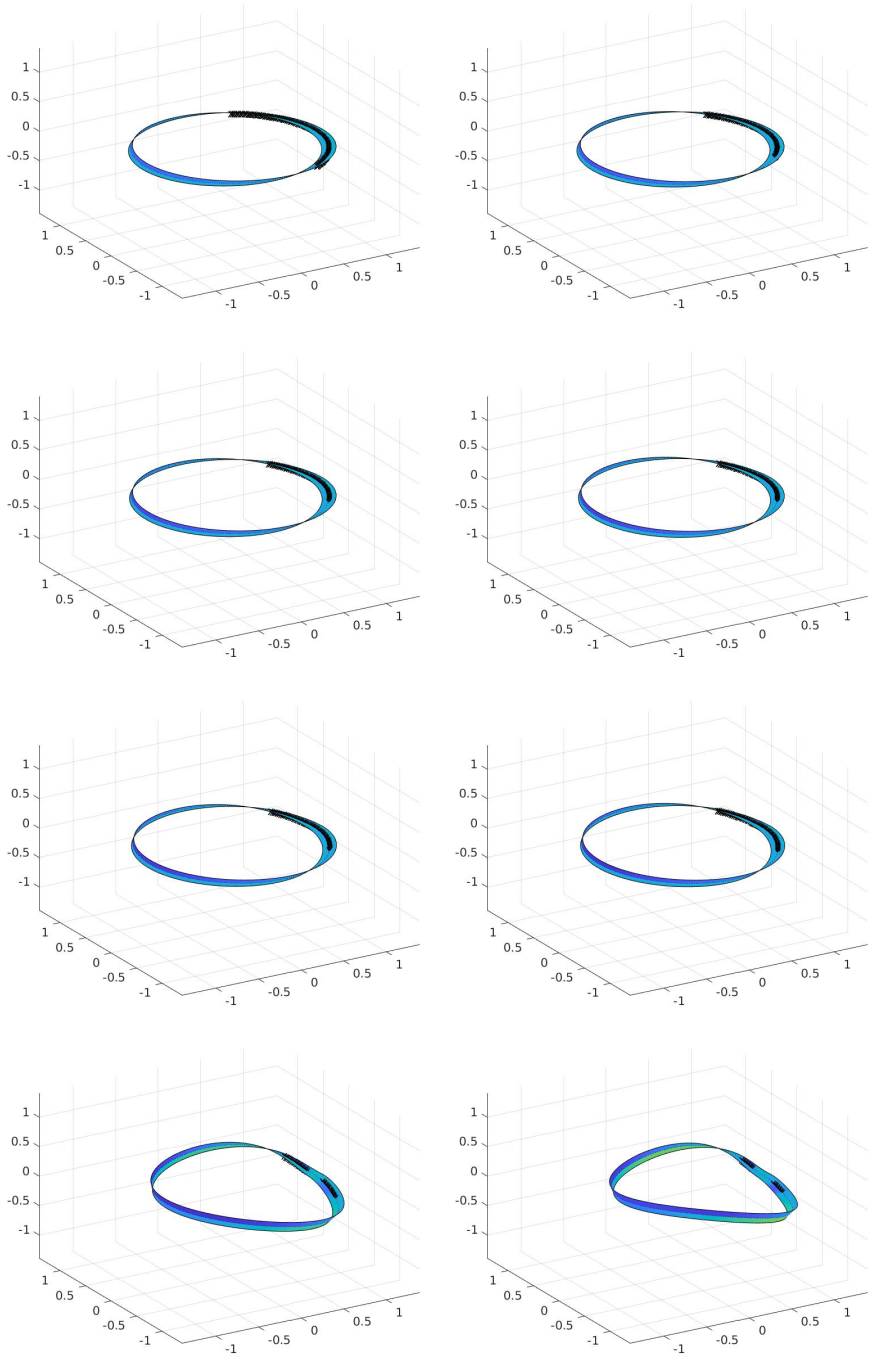

FIG. 1. *Snapshots of the discrete gradient flow in Example* 6.1 *after* $k = 0, 102, 204, 306, 408, 510, 2448, 5100$ *iterations leading to a Möbius strip, colored by curvature and torsion; crosses indicate where torsion dominates curvature.*

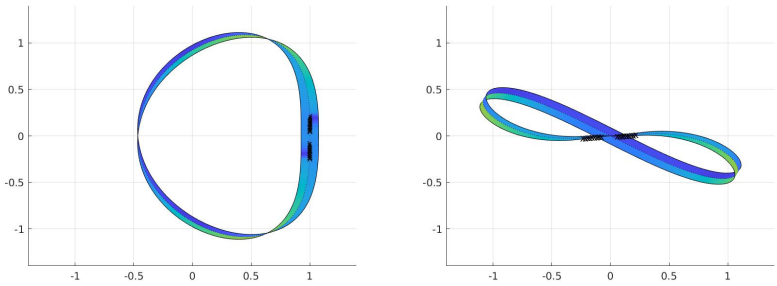

FIG. 2. *Nearly stationary configuration in Example* 6.1 *from different perspectives colored by curvature and torsion; crosses indicate where torsion dominates curvature.*

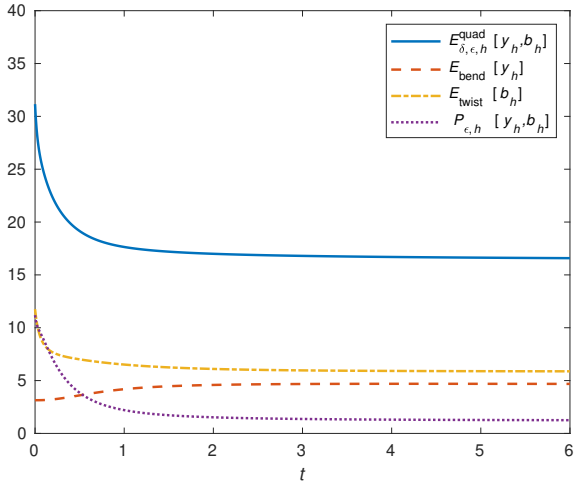

FIG. 3. *Energy decay in Example* 6.1 *accompanied by an increase of bending energy; twist energy and penalty functional decay monotonically.*

become nearly stationary; cf. Figure 3. The discrete director fields b_h^0 and b_h^k with $k = 5100$ are displayed at selected deformed nodes in Figure 4. An experimental convergence behavior of the stationary energies for discretizations with $h = L/N$, $N = 80, 160, 320, 640$ is provided in Table 1. We observe that the energies increase with finer resolutions, and their differences become smaller. These results also indicate that the scheme does not tend to get stuck at local minima.

6.3. Twisted helix. A helix is a canonical example of a twisted band. We consider here the evolution from a helical configuration where the torsion is inconsistent with the winding of the helix.

Example 6.2 (twisted helical ribbon). Let $L = 2\pi$, and define for $x \in (0, L)$

$$y_0(x) = \big(cx, d\cos(\beta x), d\sin(\beta x)\big),$$

where $c = 0.95$ and $d = (1 - c^2)^{1/2}/\beta$ with $\beta = 2$, and with $\alpha = 1$ let

$$b_0 = \Pi_{S_1}\big[\cos(\alpha\cdot)(y_0' \times n_0) \times y_0' + \sin(\alpha\cdot)y_0' \times n_0\big],$$

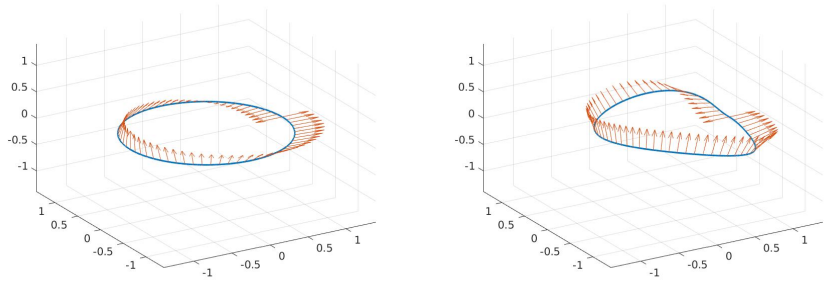

FIG. 4. *Initial and nearly stationary director fields on the deformed centerline in Example* 6.1*; the vectors at every fourth node are displayed.*

TABLE 1
Stationary energy values in Example 6.1 *for different mesh-sizes* $h = L/N$.

$N \sim h^{-1}$	80	160	320	640
$E^{\mathrm{quad}}_{\delta,\varepsilon,h}[y_h, b_h]$	14.8540	15.8817	16.5832	17.0582

TABLE 2
Stationary energy values in Example 6.2 *for different mesh-sizes* $h = L/N$.

$N \sim h^{-1}$	80	160	320	640
$E^{\mathrm{quad}}_{\delta,\varepsilon,h}[y_h, b_h]$	27.7554	26.5432	26.3554	26.4050

where $n_0 = [y_0']_2^{\perp}$ (cf. Example 6.1), and $\Pi_{S_1} : \mathbb{R}^3 \setminus \{0\} \to \mathbb{R}^3$ denotes the projection onto the unit sphere.

The application of Algorithm 5.1 to the initial data defined by Example 6.2 leads to the snapshots displayed in Figure 5. In contrast to Example 6.1, we observe in Example 6.2 that in the nearly stationary configuration curvature is dominated by torsion along the entire centerline; cf. Figure 6. Interestingly, this is also the case for the initial configuration but changes during the evolution. The discrete, dimensionally reduced energy, the twist energy, and the penalty value decrease monotonically during the evolution while the bending energy shows a moderate increase, as can be seen in the plot of Figure 7. The initial and nearly stationary director fields are displayed in Figure 8. The stationary energies for a sequence of refined partitions are provided in Table 2. In comparison with Example 6.1, we observe here a nonmonotone behavior and smaller differences.

Acknowledgment. The author acknowledges stimulating discussions with Peter Hornung.

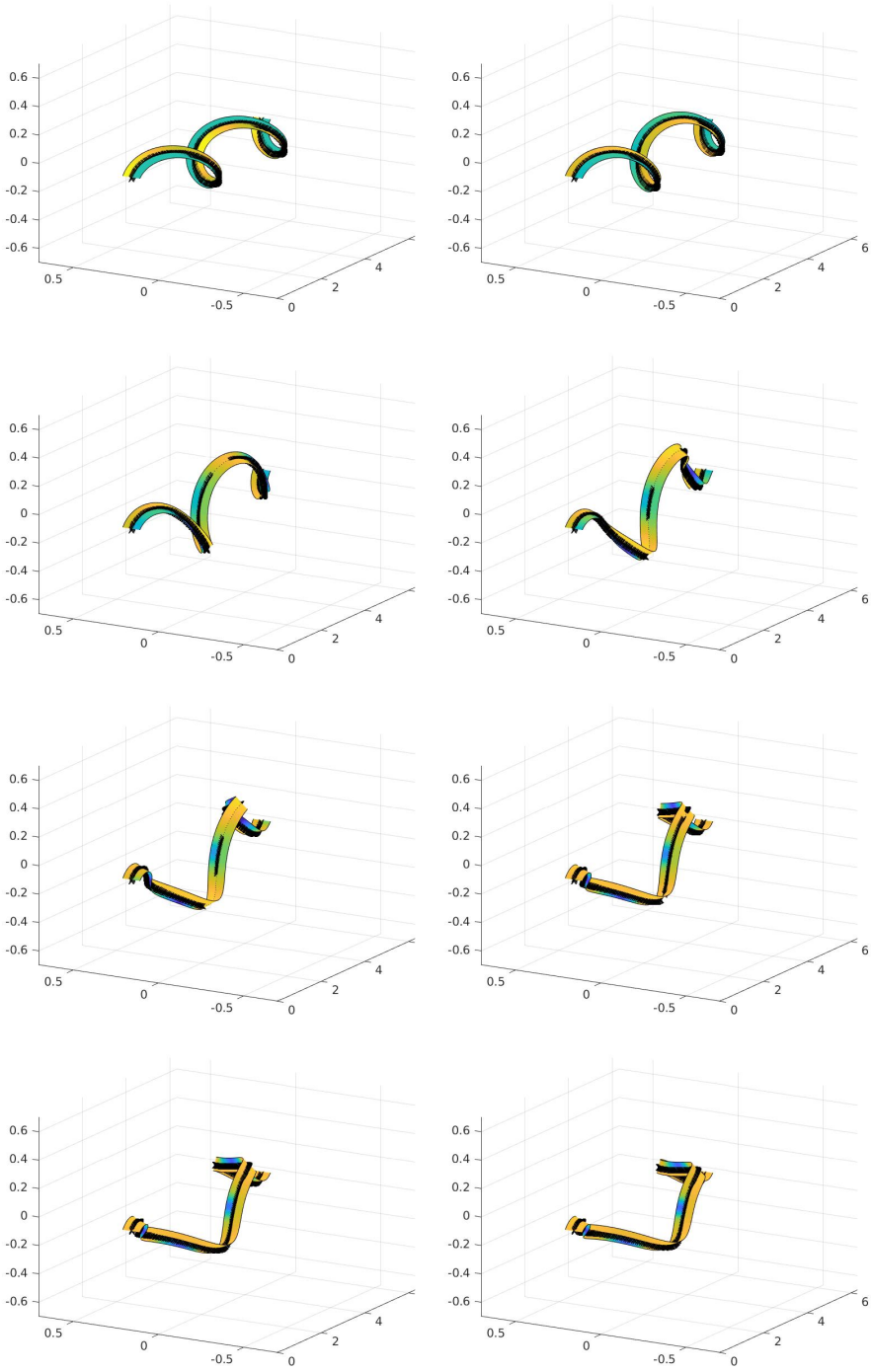

FIG. 5. *Snapshots of the discrete gradient flow in Example* 6.2 *after* $k = 0, 408, 816, 1224, 1632, 2040, 2448, 5092$ *iterations starting from a helix, colored by curvature and torsion; crosses indicate where torsion dominates curvature.*

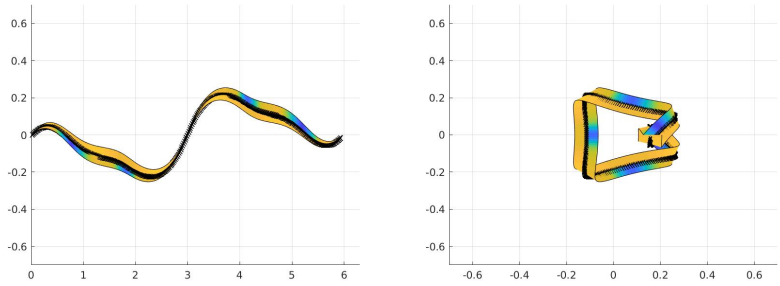

FIG. 6. *Nearly stationary configuration in Example* 6.2 *from different perspectives colored by curvature and torsion; crosses indicate where torsion dominates curvature.*

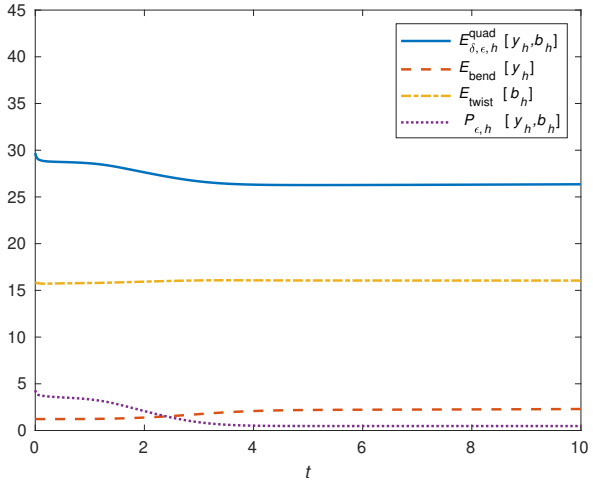

FIG. 7. *Energy decay in Example* 6.2 *accompanied by a small increase of bending energy; twist energy and penalty functional decay monotonically.*

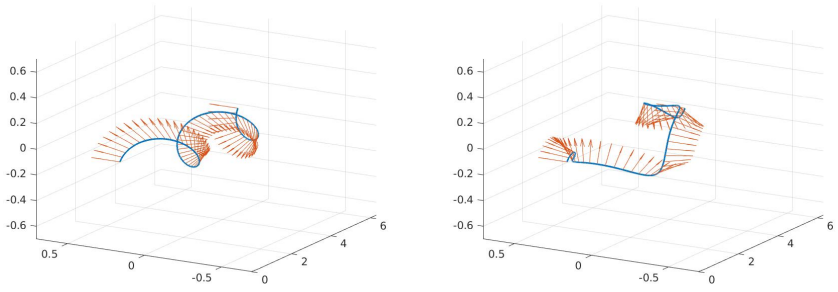

FIG. 8. *Initial and nearly stationary director fields on the deformed centerline in Example* 6.2*; the vectors at every fourth node are displayed.*

REFERENCES

[1] B. Audoly and K. A. Seffen, *Buckling of naturally curved elastic strips: The ribbon model makes a difference*, J. Elasticity, 119 (2015), pp. 293–320, https://doi.org/10.1007/s10659-015-9520-y.

[2] S. Bartels, *Approximation of large bending isometries with discrete Kirchhoff triangles*, SIAM J. Numer. Anal., 51 (2013), pp. 516–525, https://doi.org/10.1137/110855405.

[3] S. Bartels, *Numerical Methods for Nonlinear Partial Differential Equations*, Springer Ser. Comput. Math. 47, Springer, Cham, 2015, https://doi.org/10.1007/978-3-319-13797-1.

[4] S. Bartels and P. Hornung, *Bending paper and the Möbius strip*, J. Elasticity, 119 (2015), pp. 113–136, https://doi.org/10.1007/s10659-014-9501-6.

[5] S. Bartels and P. Reiter, *Numerical Solution of a Bending-Torsion Model for Elastic Rods*, preprint, https://arxiv.org/abs/1911.07024, 2019.

[6] L. Freddi, P. Hornung, M. G. Mora, and R. Paroni, *A corrected Sadowsky functional for inextensible elastic ribbons*, J. Elasticity, 123 (2016), pp. 125–136, https://doi.org/10.1007/s10659-015-9551-4.

[7] L. Freddi, P. Hornung, M. G. Mora, and R. Paroni, in preparation, 2019.

[8] G. Friesecke, R. D. James, and S. Müller, *A theorem on geometric rigidity and the derivation of nonlinear plate theory from three-dimensional elasticity*, Comm. Pure Appl. Math., 55 (2002), pp. 1461–1506, https://doi.org/10.1002/cpa.10048.

[9] P. Hornung, *Deformations of Framed Curves with Boundary Conditions*, preprint, http://wwwpub.zih.tu-dresden.de/~phornung/publications.html, 2020.

[10] N. O. Kirby and E. Fried, *Gamma-limit of a model for the elastic energy of an inextensible ribbon*, J. Elasticity, 119 (2015), pp. 35–47, https://doi.org/10.1007/s10659-014-9475-4.

[11] M. G. Mora and S. Müller, *Derivation of the nonlinear bending-torsion theory for inextensible rods by* Γ*-convergence*, Calc. Var. Partial Differential Equations, 18 (2003), pp. 287–305, https://doi.org/10.1007/s00526-003-0204-2.

[12] M. Sadowsky, *Ein elementarer Beweis für die Existenz eines abwickelbaren Möbiusschen Bandes und die Zurückführung des geometrischen Problems auf ein Variationsproblem*, Sitzungsber. Preuss. Akad. Wiss., Berlin, Mitteilung vom 26 Juni, 1930, pp. 412–415.

[13] M. Sadowsky, *Theorie der elastisch biegsamen undehnbaren Bänder mit Anwendungen auf das Möbiussche Band*, Verh. 3. Int. Kongr. Tech. Mech., 2 (1930), pp. 444–451.

[14] E. L. Starostin and G. H. M. van der Heijden, *The shape of a Möbius strip*, Nature Materials, 6 (2007), pp. 563–567.

[15] G. Stoychev, S. Zakharchenko, S. Turcaud, J. W. C. Dunlop, and L. Ionov, *Shape-programmed folding of stimuli-responsive polymer bilayers*, ACS Nano, 6 (2012), pp. 3925–3934, https://doi.org/10.1021/nn300079f.

[16] W. Wunderlich, *Über ein abwickelbares Möbiusband*, Monatsh. Math., 66 (1962), pp. 276–289, https://doi.org/10.1007/BF01299052.